# Metallic $ReO_3$ Nanoparticles

**Kanishka Biswas[†,‡] and C. N. R. Rao*[,†,‡]**

*Chemistry and Physics of Materials Unit and CSIR Centre of Excellence in Chemistry, Jawaharlal Nehru Centre for Advanced Scientific Research Jakkur P. O., Bangalore-560064, India, and Solid State and Structural Chemistry Unit, Indian Institute of Science, Bangalore-560012, India*

*Received: October 5, 2005; In Final Form: November 18, 2005*

$ReO_3$ nanoparticles in the diameter range of 8.5−32.5 nm have been prepared by decomposition of the $Re_2O_7$−dioxane complex under solvothermal conditions and characterized by X-ray diffraction, electron microscopy, optical spectroscopy, and scanning probe microscopy. The nanoparticles have the cubic ($Pm\bar{3}m$ {221} space group) structure with the lattice parameter increasing with decreasing size. The particles are metallic and show a plasmon band around 520 nm, which becomes blue-shifted with a decrease in size. The metallicity of the nanoparticles is also confirmed by tunneling conductance measurements. The nanoparticles show paramagnetic or diamagnetic behavior depending on the size, with evidence for superparamagnetism at low temperatures when the size is small.

## Introduction

Nanocrystals and quantum dots constitute an important family of zero-dimensional nanomaterials. A variety of nanocrystals has been investigated in recent years.[1] In particular, nanocrystals of different trasition metal oxides have been prepared and characterized by several workers.[2] Transition metal oxides constitute the most interesting class of materials because of the wide range of properties and phenomena exhibited by them.[3] One of the most interesting among the transition metal oxides is $ReO_3$, which created a sensation in the solid-state literature when it was shown to be metallic with a conductivity close to that of copper.[3,4] We considered it of significance to prepare nanoparicles of $ReO_3$ and characterize them through their magnetic, electrical, and optical properties. For this purpose, we had to find an appropriate synthetic procedure. Since $ReO_3$ nanoparticles cannot be obtained directly from $Re_2O_7$ by simple means, we have used the $Re_2O_7$−dioxane complex as the precursor and obtained the $ReO_3$ nanoparticles by the thermal decomposition of the precursor under solvothemal conditions. In this paper, we report the successful synthesis of $ReO_3$ nanoparticles and their characterization.

## Experimental Procedures

To prepare $ReO_3$ nanoparticles, the rhenium (VII) oxide−dioxane complex, $Re_2O_7$−$(C_4H_8O_2)_x$, was prepared as the starting material following the literature procedure.[5,6] In a typical preparation, 0.05 g (0.24 mmol) of $Re_2O_7$ was taken in a 10 mL round-bottomed flask, to which 0.5 mL (5.86 mmol) of anhydrous 1,4-dioxane was added. The contents of the flask were gently warmed in a water bath at 70 °C to obtain a colorless solution. The solution was placed in an ice bath, and the frozen mass was allowed to warm to room temperature. The rhenium (VII) oxide−dioxane complex (RDC) precipitated out as a dense, pearl gray deposit. The freezing−melting operation was repeated to ensure complete separation of the complex. The colorless supernatant liquid was removed by decantation. The complex was unstable in open air at room temperature and was therefore dissolved in ethanol for later use. The ethanol solution was green. In Figure 1a, we show the electronic absorption spectrum of the $Re_2O_7$−dioxane complex dissolved in ethanol as well as of $Re_2O_7$ dissolved in acetone. In Figure 1b, we show the spectrum of $Re_2O_7$ in the solid phase. The dioxane complex shows a sharp band around 335 nm, unlike solid $Re_2O_7$, which contains both metal−oxygen octahedra and tetrahedra.[7] Interestingly, the greenish solution of $Re_2O_7$ dissolved in acetone gives an absorption spectrum similar to that of the dioxane complex (see Figure 1a). It is possible that there is only one type of metal coordination in RDC as well as in $Re_2O_7$−acetone.

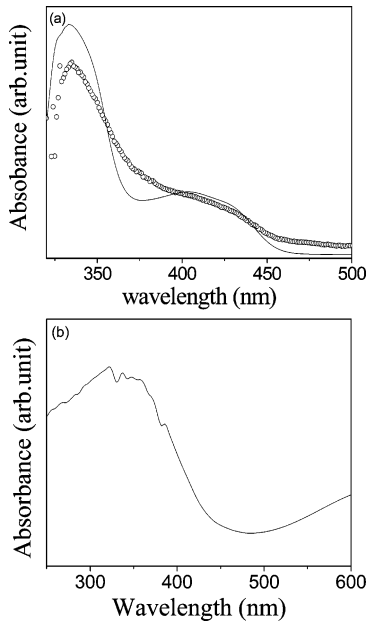


**Figure 1.** UV−vis spectra of (a) $Re_2O_7$−dioxane complex dissolved in ethanol (open circle) and $Re_2O_7$ dissolved in acetone (solid line) and (b) solid $Re_2O_7$.

* Corresponding author. Fax: (+91) 80 22082760. E-mail: cnrrao@jncasr.ac.in.

† Jawaharlal Nehru Centre for Advanced Scientific Research Jakkur P. O.

‡ Indian Institute of Science.

10.1021/jp055670b CCC: $33.50 
Published on Web 12/21/2005

$ReO_3$ nanoparticles were prepared by the decomposition of the RDC at 200 °C in toluene under solvothermal conditions. In a typical synthesis, the RDC dissolved in 2 mL (30.08 mmol) of ethanol was taken in 45 mL of toluene and sealed in a Teflon-lined stainless steel autoclave of 80 mL capacity (at 70% filling fraction). The autoclave was placed inside a preheated air-oven at 200 °C for 4 h and allowed to cool to room temperature. A red solid dispersed in toluene was obtained as the product. To this dispersion, excess ethanol was added and kept overnight. The red $ReO_3$ nanoparticles (17 nm diameter) were washed several times with acetone. The sample was dried in an air-oven at 50 °C for 1 h. The nanoparticles could be redispersed in toluene, hexane, or carbon tetrachloride.

To vary the particle size of $ReO_3$, the concentration of RDC and the reaction time were varied, keeping the amount of toluene and the filling fraction of the autoclave constant. Higher temperatures, longer heating times, and higher RDC concentrations generally yielded particles of larger sizes. Nanoparticles of different diameters were obtained as follows: 8.5 nm: RDC dissolved in 2 mL (30.08 mmol) of ethanol prepared from 0.01 g (0.048 mmol) of $Re_2O_7$ and 0.1 mL (1.17 mmol) of dioxane, 200 °C, 8 h; 12 nm: RDC dissolved in 2 mL (30.08 mmol) of ethanol prepared by 0.025 g (0.12 mmol) of $Re_2O_7$ and 0.25 mL (2.93 mmol) of dioxane, 200 °C, 4 h; 17 nm: RDC dissolved in 2 mL (30.08 mmol) of ethanol prepared from 0.05 g (0.24 mmol) of $Re_2O_7$ and 0.5 mL (5.83 mmol) of dioxane, 200 °C, 4 h; 32.5 nm: RDC dissolved in 2 mL (30.08 mmol) of ethanol prepared from 0.05 g (0.24 mmol) of $Re_2O_7$ and 0.5 mL (5.83 mmol) of dioxane, 220 °C, 4 h.

The $ReO_3$ nanoparticles were characterized by powder X-ray diffraction (XRD) using a Phillips X'Pert diffractometer employing the Bragg−Brentano configuration. For transmission electron microscopy (TEM), hexane or carbon tetrachloride dispersions of the nanoparticles were taken on holey carbon-coated Cu grids, and the grids dried in air. The grids were examined using a JEOL (JEM3010) microscope operating with an accelerating voltage of 300 kV. Samples of the as-prepared nanoparticles were subject to the magnetic characterization using a vibrating sample magnetometer in the Physical Property Measurement System (Quantum Design). Electronic absorption spectra were recorded using a Perkin-Elmer spectrometer.

Scanning tunneling microscopy (STM) and spectroscopy of the $ReO_3$ nanoparticles were performed at room temperature with a SPM 32 (RHK Technology) microscope. Highly oriented pyrolytic graphite (HOPG) was used as the substrate to deposit the nanocrystals. A nanocrystal suspension in carbon tetrachloride was sonicated for 60 min, after which a few drops were deposited on the substrate. The substrate was dried in air for a period of 12−14 h. Imaging and spectroscopy were carried out using electrochemically etched Au tips. To prevent tip induced damage and capture of the nanocrystal by the tip, high impedance (bias 1 V, set-point current, 1 nA) was used for imaging.

## Results and Discussion

In Figure 2, we show the X-ray diffraction patterns of $ReO_3$ nanoparticles of four different sizes. Figure 2 also gives the Rietveld profile fits along with the difference patterns obtained by using the Rietveld XND code.[8] The patterns could be indexed on the $Pm\bar{3}m$ {221} space group (JCPDS 00-24-1009). By making use of the line-widths from the Rietveld fits, the average particle sizes were estimated by using the Scherrer formula. The lattice parameters obtained from the Rietveld fits are 3.747(1), 3.748(2), 3.767(3), and 3.774(5) Å, respectively, for the 32.5, 17, 12, and 8.5 nm particles, reflecting a slight increase in the lattice parameter with the decease in particle size. The values of $R_w$, $R_{ep}$, and chi$^2$ (goodness of fit) are 0.086, 0.065, 1.24; 0.076, 0.043, 1.56; 0.075, 0.041, 1.76; and 0.092, 0.034, 1.42, respectively, for the 32.5, 17, 12, and 8.5 nm particles.

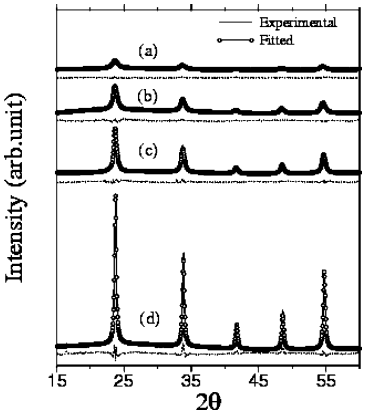


**Figure 2.** XRD patterns of the $ReO_3$ nanocrystals with average diameters of (a) 8.5, (b) 12, (c) 17, and (d) 32.5 nm along with the Rietveld fits. Difference patterns are also shown below the observed patterns.

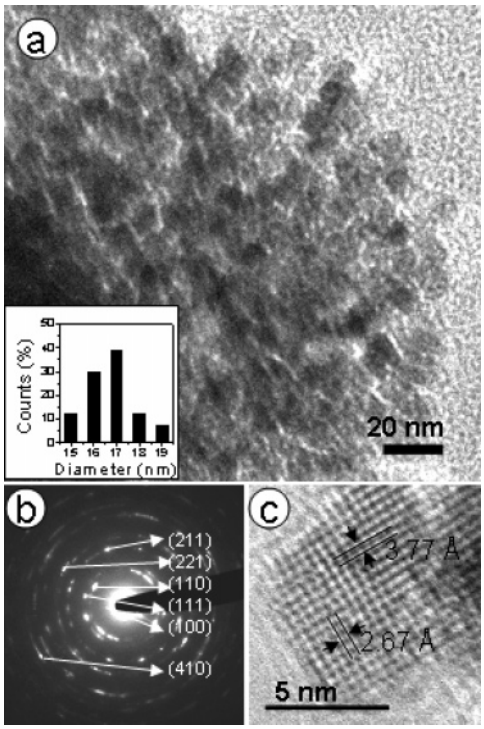


**Figure 3.** Shows (a) TEM image of 17 nm $ReO_3$ nanocrystals with size distribution histogram as an inset, (b) single particle HREM image of the 8.5 nm particle, and (c) SAED patterns of 17 nm nanoparticles.

A TEM image of the $ReO_3$ nanoparticles with an average diameter of 17 nm is shown in Figure 3a. The particles are reasonably monodisperse as seen from the histogram shown in the inset of the Figure 3a. An indexed selected area electron diffraction (SAED) pattern of the 17 nm sample is shown in Figure 3b. In Figure 3c, we show the high-resolution electron microscope image of a 8.5 nm nanoparticle. The lattice spacings of 3.75 and 2.65 Å correspond to the (100) and (110) interplanar distances, respectively.

$ReO_3$ is known to exhibit a plasmon absorption band around 520 nm the electronic absorption spectrum.[9] In Figure 4, we show the electronic absorption spectra of the $ReO_3$ nanoparticles prepared by us. The spectra clearly show that the $\lambda_{max}$ of the

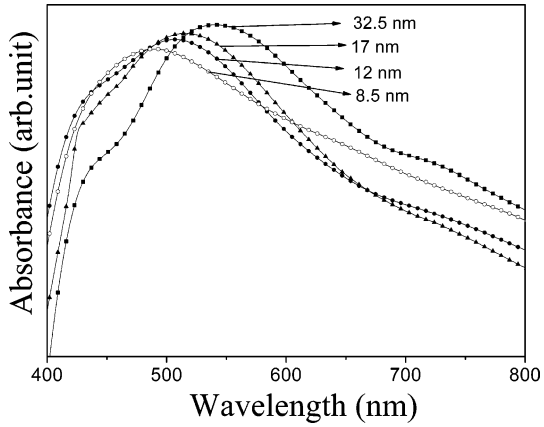


**Figure 4.** Visible spectra of the $ReO_3$ nanocrystals with average diameters of 8.5, 12, 17, and 32.5 nm.

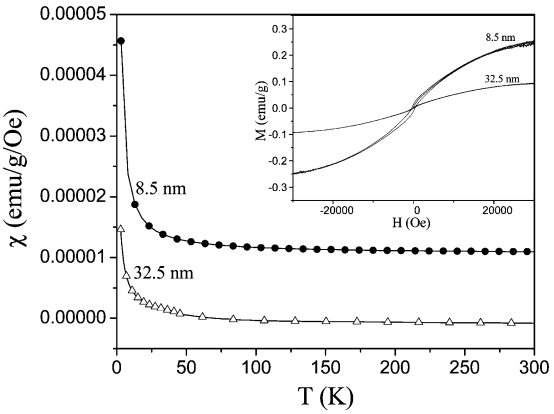


**Figure 5.** Magnetic susceptibility vs temperature curves of 8.5 and 32.5 nm particles. Inset shows the field dependence of magnetization of the 8.5 and 32.5 nm particles at 5 K.

absorption band shifts to lower wavelengths with the decrease in particle size. Thus, the $\lambda_{max}$ values are 543, 516, 507, and 488 nm, respectively, for the 32.5, 17, 12, and 8.5 nm nanocrystals. Such a blue-shift of the surface plasmon band with the decreasing particle size is observed in gold nanoparticles as well. For example, Au nanoparticles with diameters of 9 and 22 nm exhibit the plasmon bands at 512 and 528 nm, respectively.[10]

Ferretti et al.[4] reported $ReO_3$ to be diamagnetic, while Quinn and Neiswander[11] reported it to be paramagnetic. We have measured the magnetic susceptibility of the 8.5 and 32.5 nm nanoparticles over the 2−300 K range, and the results are shown in Figure 5. The 32.5 nm particles are diamagnetic at room temperature, while the 8.5 nm particles are paramagnetic. The value of the magnetization of the 8.5 nm particles is generally higher than that of the 32.5 nm particles, probably due to the presence of a larger number of uncompensated surface spins in the smaller particles. The inset in Figure 5 shows the variation of the magnetization with field measured at 5 K for the 8.5 and 32.5 nm samples. There is a distinct magnetic hysteresis in the case of the 8.5 nm particles, which disappears above 20 K. Such hysteresis arises from ferromagnetic interactions among the uncompensated spins in the small particles of antiferromagnetic materials such as CoO.[12] Such small oxide particles are superparamagnetic at low temperatures and exhibit magnetic hysteresis below a blocking temperature.[13] The hysteretic behavior of paramagnetic $ReO_3$ is interesting indeed.

Figure 6a,b shows typical STM images of $ReO_3$ nanocrystals. Most of the nanocrystals have sizes in the 8−10 nm range as seen in Figure 6a. Figure 6b shows a one-dimensional chain

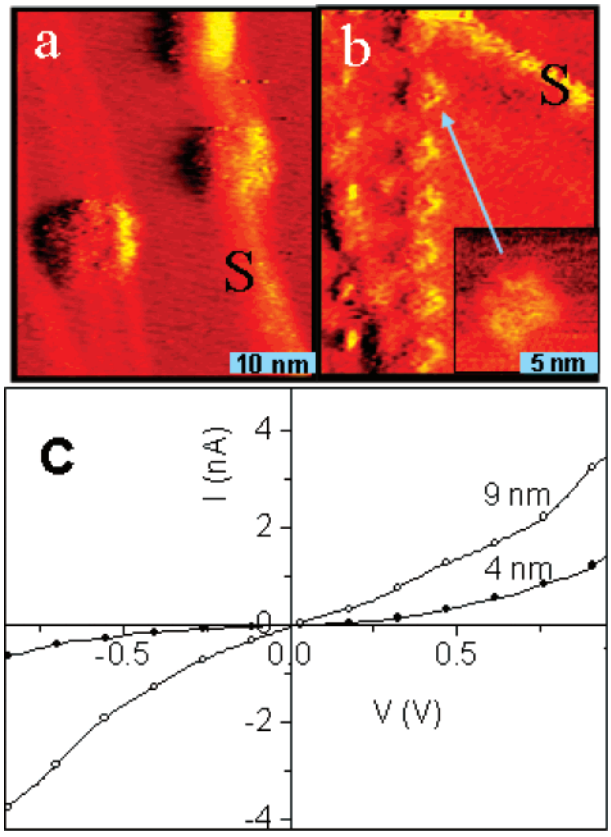


**Figure 6.** STM images of (a) 9 nm $ReO_3$ nanocrystals and (b) 1-D self-assembly of smaller nanocrystals (4 nm). The images were acquired at 1 V bias voltage and 1 nA tunneling current. S denotes steps on HOPG. (c) I−V data for the nanocrystals shown in panels a and b.

arrangement formed by 4 nm particles. Figure 6c displays the I−V characteristics of the nanocrystals, acquired under identical conditions at a bias-voltage of 1 V and a set-point current of 1 nA. The I−V curves are smooth and symmetric about the zero bias voltage. The 9 nm nanocrystals exhibit tunneling currents, which are 4 times that of the clean substrate. However, as the size of the nanocrystals decreases, the resistance increases. We do not, however, observe a band gap in the particles.

The results discussed previously clearly demonstrate that $ReO_3$ nanoparticles can indeed be prepared satisfactorily by the decomposition of RDC under solvothermal conditions. It is noteworthy that nanoparticles in the size range of 8−33 nm prepared by us show metallic behavior as characterized by the plasmon resonance. Furthermore, while the average magnetic properties are as expected, being diamagnetic or paramagnetic, the low-temperature hysteresis is an unusual feature. It should be possible to use $ReO_3$ nanoparticles in place of nanoparticles of conventional metals such as gold and platinum.

## Conclusions

In conclusion, we have successfully synthesized metallic $ReO_3$ nanoparticles by the decomposition of the $Re_2O_7$−dioxane complex under solvothermal conditions. We have been able to obtain $ReO_3$ nanoparticles from the $Re_2O_7$−acetone complex under solvothemal conditions. This procedure needs to be examined in greater detail. The $Re_2O_7$−acetone complex appears to be a new precursor for $ReO_3$. The nanoparticles exhibit the characteristic plasmon band, which is size-dependent, besides showing weakly paramagnetic behavior at ordinary temperatures and magnetic hysteresis at low temperatures when the particle size is small.

**Acknowledgment.** We thank Mr. Ujjal K. Gautam for assistance with STM measurements.

## References and Notes

(1) (a) Rao, C. N. R., Mueller, A., Cheetham, A. K., Eds. *The Chemistry of Nanomaterials*; Wiley-VCH: Weinheim, 2004. (b) Schmid, G. *Nanoparticles: Theory to Application*; Wiley-VCH: Weinheim, 2004. (c) Burda, C.; Chen, X.; Narayanan, R.; El-Sayed, M. A. *Chem. Rev.* **2005**, *105*, 1025.

(2) Seshadri, R. In *The Chemistry of Nanomaterials*; Rao, C. N. R., Mueller, A., Cheetham, A. K., Eds.; Wiley-VCH: Weinheim, 2004; Vol. 1, p 94.

(3) Rao, C. N. R.; Raveau, B. *Transition Metal Oxides*, 2nd ed.; Wiley-VCH: Weinheim, 1995.

(4) Ferretti, A.; Rogers, D. B.; Goodenough, J. B. *J. Phys. Chem. Solids* **1965**, *26*, 2007.

(5) Nechamkin, H.; Kurtz, A. N.; Hiskey, C. F. *J. Am. Chem. Soc*. **1951**, *73*, 2828.

(6) Audrieth, L. F. *Inorg. Synth.* **1950**, *3*, 187.

(7) Krebs, B.; Muller, A.; Beyer, H. H. *Inorg. Chem*. **1969**, *8*, 436.

(8) Berar, J.-F.; Garnier, P. *NIST Spec. Publ*. **1992**, *846*, 212.

(9) Edreva-Kardzhieva, R.; Andreev, A. A. *Z. Neorg. Khim.* **1977**, *22*, 2007.

(10) Fukuoka, A.; Araki, H.; Kimura, J.; Sakamoto, Y.; Higuchi, T.; Sugimoto, N.; Ichikawa, M. *J. Mater. Chem.* **2004**, *14*, 752.

(11) Quinn, R. K.; Neiswander, P. G. *Mater. Res. Bull*. **1970**, *5*, 329.

(12) Ghosh, M.; Sampatkumaran, E. V.; Rao, C. N. R. *Chem. Mater*. **2005**, *17*, 2348.

(13) (a) Makhlouf, S. A.; Parker, F. T.; Spada, F. E.; Berkowitz, A. E. *J. Appl. Phys*. **1997**, *81*, 5561. (b) Park, J.; An, K.; Hwang, Y.; Park, J.-G.; Noh, H.-J.; Kim, J.-Y.; Park, J.-H.; Hwang, N.-M.; Hyeon, T. *Nat. Mater*. **2004**, *3*, 891. (c) Bødker, F.; Hansen, M. F.; Koch, C. B.; Mørup, S. *J. Magn. Magn. Mater*. **2000**, *221*, 32. (d) Kodama, R. H.; Makhlouf, S. A.; Berkowitz, A. E. *Phys. Rev. Lett*. **1997**, *79*, 1393.